Development of surrogate correlation models to predict trace organic contaminant oxidation and microbial inactivation during ozonation

Daniel Gerrity [a,b,c,*], Sujanie Gamage [c], Darryl Jones [d], Gregory V. Korshin [e], Yunho Lee [f,g], Aleksey Pisarenko [c], Rebecca A. Trenholm [c], Urs von Gunten [g,h], Eric C. Wert [c], Shane A. Snyder [d]

[a] Department of Civil and Environmental Engineering and Construction, University of Nevada, Las Vegas, Box 454015, 4505 S. Maryland Parkway, Las Vegas, NV 89154-4015, United States
[b] Trussell Technologies, Inc., 232 North Lake Avenue, Suite 300, Pasadena, CA 91101, United States
[c] Applied Research and Development Center, Southern Nevada Water Authority, River Mountain Water Treatment Facility, P.O. Box 99954, Las Vegas, NV 89193-9954, United States
[d] Department of Chemical and Environmental Engineering, University of Arizona, 1133 E. James E. Rogers Way, Harshbarger 108, Tucson, AZ 85721-0011, United States
[e] Civil & Environmental Engineering, University of Washington, 201 More Hall, Box 352700, Seattle, WA 98195-2700, United States
[f] School of Environmental Science and Engineering, Gwangju Institute of Science and Technology (GIST), 123, Oryong-dong, Buk-gu, Gwangju 500-712, Republic of Korea
[g] Eawag, Swiss Federal Institute of Aquatic Science and Technology, Ueberlandstrasse 133, P.O. Box 611, 8600 Duebendorf, Switzerland
[h] School of Architecture, Civil, and Environmental Engineering (ENAC), Ecole Polytechnique Federale de Lausanne, CH-1015 Lausanne, Switzerland

ARTICLE INFO

ABSTRACT

The performance of ozonation in wastewater depends on water quality and the ability to form hydroxyl radicals (•OH) to meet disinfection or contaminant transformation objectives. Since there are no on-line methods to assess ozone and •OH exposure in wastewater, many agencies are now embracing indicator frameworks and surrogate monitoring for regulatory compliance. Two of the most promising surrogate parameters for ozone-based treatment of secondary and tertiary wastewater effluents are differential UV$_{254}$ absorbance

Abbreviations: AFU, arbitrary fluorescence unit; AOP, advanced oxidation process; AWWTP, Australian (anonymous) Wastewater Treatment Plant; BAC, biological activated carbon; BDF, buffered demand free; CCWRD, Clark County Water Reclamation District; CDPH, California Department of Public Health; CFU, colony forming unit; CLV, City of Las Vegas; CT, concentration × time (as in disinfection); DEET, N,N-diethyl-meta-toluamide; EDC, endocrine disrupting compound; EEM, excitation—emission matrix; EfOM, effluent organic matter; FAT, full advanced treatment; GCGA, Gwinnett County Georgia; GC—MS, gas chromatography mass spectrometry; IPR, indirect potable reuse; KOWWTP, Kloten—Opfikon Wastewater Treatment Plant; LC—MS, liquid chromatography mass spectrometry; LWWTP, Lausanne Wastewater Treatment Plant; MBR, membrane bioreactor; MPN, most probable number; MRL, method reporting limit; MWRDGC, Metropolitan Water Reclamation District of Greater Chicago; pCBA, para-chlorobenzoic acid; IPR, indirect potable reuse; PCU, Pinellas County Utilities; PEG, polyethylene glycol; PFU, plaque forming unit; PPCPs, pharmaceuticals and personal care products; RWWTP, Regensdorf (Wüeri) Wastewater Treatment Plant; TCEP, tris-(2-chloroethyl)-phosphate; TF, total fluorescence; TOC, total organic carbon; TOrCs, trace organic contaminants; TSA, tryptic soy agar; TSB, tryptic soy broth; U.S., United States; UV, ultraviolet; WBMWD, West Basin Municipal Water District.

* Corresponding author. Department of Civil and Environmental Engineering and Construction, University of Nevada, Las Vegas, Box 454015, 4505 S. Maryland Parkway, Las Vegas, NV 89154-4015, United States. Tel.: +1 (702) 895 3955; fax: +1 (702) 895 3936.
E-mail address: daniel.gerrity@unlv.edu (D. Gerrity).

(ΔUV_{254}) and total fluorescence (ΔTF). In the current study, empirical correlations for ΔUV_{254} and ΔTF were developed for the oxidation of 18 trace organic contaminants (TOrCs), including 1,4-dioxane, atenolol, atrazine, bisphenol A, carbamazepine, diclofenac, gemfibrozil, ibuprofen, meprobamate, naproxen, N,N-diethyl-meta-toluamide (DEET), para-chlorobenzoic acid (pCBA), phenytoin, primidone, sulfamethoxazole, triclosan, trimethoprim, and tris-(2-chloroethyl)-phosphate (TCEP) ($R^2 = 0.50–0.83$) and the inactivation of three microbial surrogates, including *Escherichia coli*, MS2, and *Bacillus subtilis* spores ($R^2 = 0.46–0.78$). Nine wastewaters were tested in laboratory systems, and eight wastewaters were evaluated at pilot- and full-scale. A predictive model for •OH exposure based on ΔUV_{254} or ΔTF was also proposed.

1. Introduction

Trace organic contaminants (TOrCs) pose a challenge for wastewater treatment facilities due to an increased awareness of their ubiquity, the ambiguity of public and aquatic health implications, the high costs associated with their quantification, and the paucity of regulatory guidance. The use of ozone for the transformation of TOrCs, including pharmaceuticals and personal care products (PPCPs) and endocrine disrupting compounds (EDCs), has been studied extensively in the literature (Huber et al., 2003, 2004; Buffle et al., 2006; Lee et al., 2008; Dodd et al., 2009; von Sonntag and von Gunten, 2012). Studies specifically addressing the efficacy of ozone for TOrC elimination, reductions in estrogenicity, and the effects on toxicity have also been performed in pilot- and full-scale systems (Huber et al., 2005; Hollender et al., 2009; Wert et al., 2009a; Stalter et al., 2010a, 2010b; Gerrity et al., 2011a; Gerrity and Snyder, 2011; Zimmermann et al., 2011). Ozone is also effective for the inactivation of a wide range of microbial indicators and pathogens (Driedger et al., 2001; Burns et al., 2007; Gerrity et al., 2011a).

This demonstrated efficacy for TOrC mitigation and disinfection has established ozone as a viable option for wastewater treatment. Ozone-based treatment trains are also becoming increasingly popular in indirect potable reuse (IPR) applications as an alternative to membrane filtration, reverse osmosis, and UV/H_2O_2, which is described as full advanced treatment (FAT) by the California Department of Public Health (CDPH) in the United States (U.S.) (CDPH, 2011). By combining ozone with downstream biological filtration, this alternative treatment train is capable of providing a finished water quality similar to that of FAT, albeit at potentially reduced costs (Hollender et al., 2009; Reungoat et al., 2010; Stalter et al., 2010a, 2010b; Gerrity et al., 2011a; Reungoat et al., 2012; Zimmermann et al., 2011).

In wastewater applications, particularly when supplemented with hydrogen peroxide, ozonation can be considered an advanced oxidation process (AOP) due to its rapid decomposition into hydroxyl radicals (•OH). In contrast with drinking water applications (Kaiser et al., submitted for publication), there are no on-line methods to measure ozone and •OH exposure in wastewater so the "CT" approach typically associated with chlorine disinfection (i.e., the product of oxidant concentration and time) cannot be applied to estimate treatment performance. Also, frequent monitoring for TOrCs and

pathogens is a costly and time-consuming proposition. As a result, many agencies are embracing indicator frameworks and highlighting the need for surrogate monitoring (Dickenson et al., 2009). For example, CDPH recently published a revised set of draft regulations for groundwater replenishment, which outlines required removals for indicator compounds based on their chemical structures and functional groups (e.g., hydroxyl aromatic, saturated aliphatic). Although these specified removals apply only to advanced oxidation in FAT applications (i.e., reverse osmosis permeate), the framework can be applied more broadly as a TOrC mitigation baseline. In addition to the specified removals, CDPH also requires FAT facilities to identify at least one surrogate parameter that can be monitored continuously, predict the level of oxidation for the indicator compounds, and alert operators to process inefficiencies and failures. Several common water quality parameters associated with bulk organic matter, specifically differential UV absorbance (ΔUV) and total fluorescence (ΔTF), offer particularly promising solutions for this type of application.

Currently, there are few studies that describe the relationships between changes in bulk organic matter, contaminant destruction, and microbial inactivation. Studies using fluorescence as part of an analytical method to detect TOrCs are becoming more common (Camacho-Munoz et al., 2009), but the goal of these studies is inherently different than using changes in bulk organic matter to estimate oxidation efficacy. Although the high sensitivity of fluorometers offers a promising tool for detection of individual contaminants, this method is hindered by interferences from background effluent organic matter (EfOM) in wastewater applications (Fig. S1). Therefore, ΔUV—more specifically, ΔUV_{254}—and ΔTF currently offer the most promising tools to supplement existing analytical methods based on liquid or gas chromatography and mass spectrometry (LC–MS or GC–MS).

Buffle et al. (2006) proposed the use of ΔUV to determine ozone exposure in wastewater applications after observing a first-order kinetic relationship between the two parameters. Based on this concept, Bahr et al. (2007), Wert et al. (2009b), and Nanaboina and Korshin (2010) developed preliminary correlations between ΔUV_{254} and several indicator compounds and microbes. Bahr et al. (2007) presented the linear regression parameters in relation to second-order ozone and •OH rate constants. Wert et al. (2009b) indicated that ozone-susceptible target compounds (i.e., $k_{O_3} > 10^3 \, M^{-1} \, s^{-1}$) demonstrated strong

linear correlations with 0–50% reductions in UV_{254} absorbance, whereas slower-reacting compounds (i.e., $k_{O_3} < 10^3$ M^{-1} s^{-1}) correlated well with 15–65% reductions in UV_{254} absorbance. In addition to developing individual correlations for six pharmaceuticals, the study indicated that the empirical correlations were consistent between different wastewater qualities. Rosario-Ortiz et al. (2010) extended this concept to the UV/H_2O_2 advanced oxidation process and confirmed that these correlations were also consistent between different water qualities. These preliminary studies indicate that ΔUV_{254} correlations offer powerful, robust, and straightforward tools that can easily be incorporated into full-scale applications.

Several studies have expanded on this preliminary research to incorporate both commercially available and innovative technologies. Pisarenko et al. (2012) developed a set of TOrC correlations based on ΔUV_{254} and ΔTF using a pilot-scale O_3/H_2O_2 reactor (HiPOx®, APTwater, Long Beach, CA), while Gerrity et al. (2010) illustrated how the ΔUV_{254} correlation concept can be applied to novel forms of advanced oxidation, specifically nonthermal plasma (AquaPure, Petach-Tikva, Israel). Therefore, the existing literature offers the following conclusions: (1) ΔUV and ΔTF are strongly correlated with the elimination of aromatic and non-aromatic TOrCs, (2) each compound has a unique set of regression parameters related to its second-order rate constants for reactions with various oxidants, (3) unit processes with different oxidation mechanisms (e.g., ozone/H_2O_2 vs. UV/H_2O_2) also have unique sets of correlations, and (4) the correlations for specific contaminants and oxidation processes are consistent between different secondary or tertiary effluents.

The objective of the current study was to expand on this foundation by developing a more comprehensive database of bench-scale correlations (i.e., increase the number of contaminants and matrices), validating those same correlations at pilot- and full-scale, and illustrating how the concept can be integrated into an actual treatment train to provide real-time, on-line monitoring of process performance. This study incorporated 18 trace organic contaminants, three microbial surrogates, nine sets of bench-scale experiments, four independent pilot-scale validations, and one full-scale validation. A commercially available on-line UV absorbance analyzer was also integrated into the study. Ultimately, this database can be integrated into the software of emerging absorbance and fluorescence technologies to allow for optimization of dosing conditions and to provide real-time estimates of contaminant oxidation and disinfection.

2. Materials and methods

2.1. Bench-scale experiments

Unfiltered secondary effluent was collected from nine wastewater treatment facilities, as described in Table 1. For the five wastewaters from the U.S., a portion of the secondary effluent was filtered in series through 10-μm and 0.5-μm (nominal) polypropylene spiral-wound cartridge filters (MicroSentry™, Shelco Filters, Middletown, CT). The four remaining wastewaters were filtered in the laboratory with 0.45-μm cellulose acetate filters. Differences in oxidation efficacy for unfiltered versus filtered secondary effluents were evaluated during the bench-scale phase. Each matrix was analyzed for a variety of general water quality parameters (Table 1) to characterize the matrices and determine the appropriate ozone and H_2O_2 dosing conditions.

Table 1 – Summary of average water quality data for the bench- (filtered), pilot-, and full-scale experiments.

Sample ID	Location	pH	TOC mg/L	UV_{254} cm^{-1}	TF AFU	Alkalinity mg/L as CaCO$_3$	NH$_3$ mg-N/L	NO$_3$ mg-N/L	NO$_2$ mg-N/L
Secondary effluents for bench-scale experiments (after laboratory filtration)									
CCWRD	Nevada	6.9	7.6	0.146	38,874	123	0.09	14.0	0.06
MWRDGC	Illinois	7.6	6.9	0.131	37,712	134	0.07	9.10	<0.05
WBMWD	California	7.3	18.0	0.268	94,807	332	46.9	0.11	0.17
PCU	Florida	7.3	7.2	0.187	53,996	205	0.02	7.70	<0.05
GCGA	Georgia	7.3	6.3	0.130	34,795	169	5.80	8.60	0.30
LWWTP	Switzerland	7.2	6.0	0.099	27,238	65	0.11	24.0	0.16
RWWTP	Switzerland	7.2	4.7	0.129	N/A	220	0.03	12.0	0.01
KOWWTP	Switzerland	7.0	4.7	0.110	N/A	145	0.02	13.2	0.07
AWWTP	Australia	7.2	7.0	0.201	51,642	105	0.09	18.0	0.05
Tertiary effluents for pilot-scale experiments									
Lit. 1[a]	Nevada	8.2	6.6	0.140	N/A	128	<0.20	13.0	<0.05
Lit. 2[a]	Florida	7.6	10.3	0.260	N/A	269	6.98	0.07	0.77
Lit. 3[a]	Colorado	7.1	10.3	0.171	N/A	101	1.28	9.70	0.40
Reno 1[b]	Nevada	6.9	5.9	0.120	32,608	90	N/A	N/A	<0.05
Reno 2[b]	Nevada	6.9	6.6	0.140	31,505	90	N/A	N/A	<0.05
Tucson	Arizona	N/A	5.6	0.157	46,496	N/A	N/A	N/A	N/A
CLV[c]	Nevada	7.3	6.0	0.130	26,988	99	<0.50	13.8	<0.10
Tertiary effluent for full-scale sampling									
Springfield	Missouri	7.9	4.9	0.116	28,782	N/A	<0.10	11.0	N/A

a Wert et al., 2009b (sand-filtered tertiary effluents).
b Gerrity et al., 2011a (Reno 1 = ultrafiltration effluent; Reno 2 = sand-filtered tertiary effluent).
c Pisarenko et al., 2012 (MBR pilot).

Separate oxidation experiments were performed for each of the major tests, as listed below, to provide sufficient sample volume for the analytical methods and to reduce potential interferences caused by spiked contaminants. Separate secondary effluent samples were spiked with (1) approximately 1 μg/L of each of the target TOrCs (3.4–5.2 nM), (2) 500 μg/L of para-chlorobenzoic acid (pCBA; 3.2 μM), (3) 1 mg/L of 1,4-dioxane (11 μM), (4) 10^7 MPN/100 mL of *Escherichia coli* 15597 (ATCC 15597), (5) 10^7 PFU/mL of the bacteriophage MS2 (ATCC 15597-B1), and (6) 10^5 CFU/100 mL of *Bacillus subtilis* spores (ATCC 23059). The *E. coli*, MS2, and *B. subtilis* spore assays were only performed on six of the nine matrices.

Bench-scale ozone tests were performed by spiking aliquots of ozone stock from a batch reactor. Nanopure water (Barnstead, Dubuque, IA) was placed inside a water-jacketed flask and cooled to 2 °C. Once cooled, 11% gaseous ozone was diffused into the water using oxygen-fed generators (U.S. experiments: model CFS-1A, Ozonia North America, Inc., Elmwood Park, NJ; international experiments: model CMG 3-3, Innovatec, Rheinbach, Germany). This configuration resulted in ozone stock solution concentrations ranging from 70 to 110 mg/L, which were measured with the indigo trisulfonate colorimetric method according to Standard Method 4500-O3 or by direct photometry at 258 nm (Hoigne and Bader, 1994). With the exception of one secondary effluent (GCGA), the study targeted mass-based ozone to total organic carbon (O_3:TOC) ratios of 0.25, 0.50, 1.0, and 1.5 (mg O_3/mg TOC). Since nitrite consumes dissolved ozone at a 1:1 mass ratio, the high nitrite concentration (0.3 mg-N/L) in the GCGA secondary effluent relative to its TOC (6.3 mg/L) resulted in corrected O_3:TOC ratios of 0.07, 0.32, 0.83, and 1.34. The effect of H_2O_2 addition was also evaluated by targeting molar H_2O_2:O_3 ratios of 0, 0.5, and 1.0. For the ozone/H_2O_2 experiments, H_2O_2 was added immediately before the addition of the ozone stock solution. All dosing ratios, bulk organic characterization, and target compound concentrations accounted for the dilution effect of the ozone spike. Upon completion of ozone decay (O_3 < 0.03 mg/L), the samples were quenched with 10 mg/L of sodium thiosulfate to eliminate any residual H_2O_2, preserved with 1 g/L of sodium azide, and stored at 4 °C prior to analysis.

2.2. Pilot-scale validation

The results from the bench-scale experiments were compared with an independent pilot-scale data set from the literature (Wert et al., 2009b) and three pilot-scale reactors associated with the current study. The ozone test matrices were comprised of five different sand-filtered effluents, one ultra-filtration filtrate, and one membrane bioreactor (MBR) filtrate. Validation data are limited for some compounds since the study from the literature only included a subset of the target compound list, and some compounds were not detected in the ambient matrices.

The Wert et al. (2009b) study evaluated pilot-scale ozonation (1 L/min) of sand-filtered tertiary effluent from three different locations in the U.S. The ozone doses ranged from 0 to 12 mg/L (no H_2O_2 addition), which corresponded to mass-based O_3:TOC ratios ranging from 0 to 1.2. For the current study, a sand-filtered tertiary effluent (Tucson, AZ) was treated with a 40-L/min pilot-scale ozone/UV/H_2O_2 reactor

(Wedeco/ITT, Herford, Germany), but it was only operated in the ozone and ozone/H_2O_2 modes for the purposes of this study. The ozone doses ranged from 0 to 9 mg/L, which corresponded to mass-based O_3:TOC ratios of 0–1.5, and molar H_2O_2:O_3 ratios of 0 and 1.0 were also tested.

A 40-L/min pilot-scale IPR treatment train (Reno, NV) comprised of ozone and biological activated carbon (BAC) was also evaluated for this study. The ozone system (HiPOx®, APTwater, Long Beach, CA) was fed with tertiary effluent after ultrafiltration for the first phase of the study and sand-filtered tertiary effluent for the second phase of the study. During both phases, ozone was dosed at 5 mg/L (mass-based O_3:TOC ratio of 0.8), and H_2O_2 was dosed at a molar H_2O_2:O_3 of 1.0 for bromate mitigation. Additional details related to the treatment train and water quality were described previously in the literature (Gerrity et al., 2011a).

The final pilot-scale system (City of Las Vegas, NV) included an 80-L/min MBR (Hydranautics, Nitto Denko, Oceanside, CA), a 40-L/min ozone system (HiPOx®), and two 40-L/min reverse osmosis skids operated in parallel (Hydranautics). Ozone doses ranged from 0 to 9 mg/L (mass-based O_3:TOC ratios of 0–2.0), and molar H_2O_2:O_3 ratios ranged from 0 to 0.5. The ozone process was evaluated with an online absorbance analyzer (spectro::lyser, s::can Messtechnik, Vienna, Austria) that was externally mounted and fed with a sidestream of process flow. Only one analyzer was available so it was adjusted manually to receive MBR filtrate and ozonated MBR filtrate at different times during the monitoring period to evaluate temporal variability. Additional details related to the operation of this pilot have also been described in the literature (Pisarenko et al., 2012).

2.3. Full-scale validation

Samples were collected from a full-scale wastewater treatment plant (Springfield, Missouri) with conventional activated sludge, sand filtration, and ozone for final disinfection. During the sampling event, the 1.14×10^5 m³/day facility was targeting an ozone production rate of approximately 544 kg/day. This corresponds to an applied ozone dose of 4.8 mg/L and a mass-based O_3:TOC ratio of approximately 1.0.

2.4. Analytical methods

2.4.1. Bulk organic matter
For TOC analysis, samples were collected in glass vials, acidified to pH <3 with hydrochloric acid, and filtered through 0.20-mm hydrophilic polypropylene filters (GHP Acro-disk, Pall Life Sciences) prior to quantification with a Shimadzu (Columbia, MD) TOC analyzer. Absorbance spectra were measured using a PerkinElmer (Waltham, MA) Lambda 45 UV–VIS Spectrometer, consistent with Standard Method 5910 B. Excitation–emission matrices (EEMs) were created using a QuantaMaster UV–Vis QM4 Steady State Spectrofluorometer (Photon Technology International, Inc., Birmingham, NJ). The spectrofluorometer included a 75-W, short-arc xenon lamp with an excitation range from 240 to 1200 nm. Data processing in MATLAB (Natick, MA) included corrections for Raman scattering, blank response, the spectral sensitivity of the lamp, and the inner filter effect (i.e., the absorbance of

the matrix). Regional integration was performed according to published literature (Chen et al., 2003) with slight modifications (Gerrity et al., 2011a) to calculate the regional and total fluorescence intensities (in arbitrary fluorescence units) for each sample.

2.4.2. Trace organic contaminants

In addition to pCBA and 1,4-dioxane, the following TOrCs were targeted in this study: atenolol, atrazine, bisphenol A, carbamazepine, N,N-diethyl-meta-toluamide (DEET), diclofenac, gemfibrozil, ibuprofen, meprobamate, musk ketone, naproxen, phenytoin, primidone, sulfamethoxazole, tris-(2-chloroethyl)-phosphate (TCEP), triclosan, and trimethoprim. Due to its high volatility, musk ketone was subsequently omitted from the study.

These target compounds were analyzed using a Symbiosis (Spark Holland, Emmen, the Netherlands) automated on-line solid phase extractor and a 4000 QTRAP triple quadrupole-linear ion trap hybrid mass spectrometer (ABSCIEX, Foster City, CA, USA). Full method descriptions and parameters, including acquisition and preparation of the TOrC spike and standard solutions, have been described previously (Trenholm et al., 2009; Gerrity et al., 2011b). The 1,4-dioxane samples were processed and analyzed by Weck Laboratories (Industry, CA) using EPA Methods 3520C and 8270M, respectively. The pCBA samples were analyzed by LC–MS/MS according to previously published methods (Vanderford et al., 2007).

The method reporting limits (MRLs) and second-order ozone and •OH rate constants for the reactions with these compounds are summarized in Table 2. The compounds were

Table 2 – Summary of target compounds and rate constants.

Compound[a]	MRL (ng/L)	k_{O_3} (M^{-1} s^{-1}), pH = 7	$k_{•OH}$ (M^{-1} s^{-1})	CDPH Classification[b]
Group 1 – High reactivity with both ozone and •OH				
Bisphenol A[h,i]	50	7×10^5	1×10^{10}	A. Hydroxy Aromatic
Carbamazepine[c]	10	3×10^5	9×10^9	C. Nonaromatic with carbon double bonds
Diclofenac[c]	25	1×10^6	8×10^9	D. Deprotonated amine
Naproxen[d,s]	25	2×10^5	1×10^{10}	E. Alkoxy polyaromatic
Sulfamethoxazole[c]	25	3×10^6	6×10^9	B. Amino/acylamino aromatic
Triclosan[e,j]	25	4×10^7	1×10^{10}	A. Hydroxy aromatic
Trimethoprim[f]	10	3×10^5	7×10^9	D. Deprotonated amine
Group 2 – Moderate reactivity with ozone and high reactivity with •OH				
Atenolol[g]	25	2×10^3	8×10^9	D. Deprotonated amine
Gemfibrozil[j,k]	10	5×10^4	1×10^{10}	F. Alkoxy aromatic
Group 3 – Moderate reactivity with both ozone and •OH				
DEET[j,l]	25	<10	5×10^9	G. Alkyl aromatic
Ibuprofen[c]	25	10	7×10^9	G. Alkyl aromatic
pCBA[p]	10,000	<0.1	5×10^9	G. Alkyl aromatic
Phenytoin[j,m]	10	<10	6×10^9	G. Alkyl aromatic
Primidone[r,j]	10	1	7×10^9	G. Alkyl aromatic
Group 4 – Low reactivity with ozone and moderate reactivity with •OH				
1,4-Dioxane[q]	500	<1	3×10^9	Alternative criterion (0.5-log removal)
Atrazine[n]	10	6	3×10^9	D. Deprotonated amine
Meprobamate[j]	10	<1	4×10^9	H. Saturated aliphatic
Group 5 – Low reactivity with both ozone and •OH				
Musk Ketone[j]	100	<1	2×10^8	I. Nitro aromatic
TCEP[j,o]	200	<1	6×10^8	H. Saturated aliphatic

a Superscripts refer to sources of O_3 (pH = 7) and •OH rate constants, respectively.
b CDPH, 2011; Groups A–G require 0.5-log removal and Groups H–I require 0.3-log removal.
c Huber et al. (2003).
d Huber et al. (2005).
e Suarez et al. (2007).
f Dodd et al. (2006).
g Benner et al. (2008).
h Deborde et al. (2005).
i Rosenfeldt and Linden (2004).
j Lee and von Gunten (2012)
k Razavi et al. (2009).
l Song et al. (2009).
m Yuan et al. (2009).
n Acero et al. (2000).
o Watts and Linden (2009).
p Katsoyiannis et al. (2011).
q Bowman et al. (2001).
r Real et al. (2009).
s Packer et al. (2003).

divided into five groups according to their relative reactivity with ozone and •OH, and they were also classified according to the recently revised CDPH Groundwater Replenishment Reuse regulations (CDPH, 2011). For context, the advanced oxidation process in every FAT facility in the State of California must demonstrate 0.5-log (groups A–G) and 0.3-log (groups H–I) removal of at least one indicator compound in each group. Alternatively, the facility may demonstrate 0.5-log removal of 1,4-dioxane in accordance with the previous draft regulations. In the context of this study, the CDPH regulations can generally be achieved by demonstrating 0.5-log removal for groups 1–3 and 0.3-log removal for groups 4–5. It is important to note that this CDPH classification scheme specifically applies to RO permeate, but it is included in this study for oxidation of secondary and tertiary effluents as a treatment baseline.

2.4.3. Microbial surrogates

E. coli samples were assayed with the 24-h Colilert (Idexx, Westbrook, ME) method using the Quanti-Tray 2000 quantification protocol. E. coli 15597 spiking stocks were propagated in log phase in tryptic soy broth (TSB). The concentrated stocks were then centrifuged, washed, and resuspended in buffered demand-free (BDF) water (Thurston-Enriquez et al., 2003). The final stocks generally contained ∼10^{10} CFU/100 mL.

The bacteriophage MS2, which is often used as a surrogate for human enteroviruses, was prepared and assayed with the double agar layer method (Adams, 1959) using antibiotic-resistant E. coli 700891 (ATCC 700891) as the bacterial host. All MS2 culture media (i.e., TSB, 0.7% tryptic soy agar (TSA) for the soft overlay, and 1.5% TSA as the solid substrate) was spiked with ampicillin and streptomycin at final concentrations of 15 mg/L to prevent growth of indigenous bacteria. Plaques were counted after 18 h of incubation at 35 °C. MS2 spiking stocks were purified with a polyethylene glycol (PEG) precipitation and Vertrel extraction before being resuspended in BDF water. This purification process was used to monodisperse the bacteriophages and remove a significant portion of the organic matter associated with the culture media, thereby reducing potential scavenging effects during the oxidation experiments (Mesquita et al., 2010). The final stocks generally contained ∼10^{11} PFU/mL.

B. subtilis spores—a surrogate for ozone-resistant microorganisms—were propagated in TSB at 35 °C and 150 rpm for 24 h, centrifuged and washed twice in BDF water to remove the nutrient-rich media, and sporulated in BDF water at 35 °C and 150 rpm for an additional 24 h. The sporulated stock was heat-shocked at 80 °C and 50 rpm for 12 min to inactivate any remaining vegetative bacteria. The spore suspension was centrifuged and washed twice in BDF water in order to create
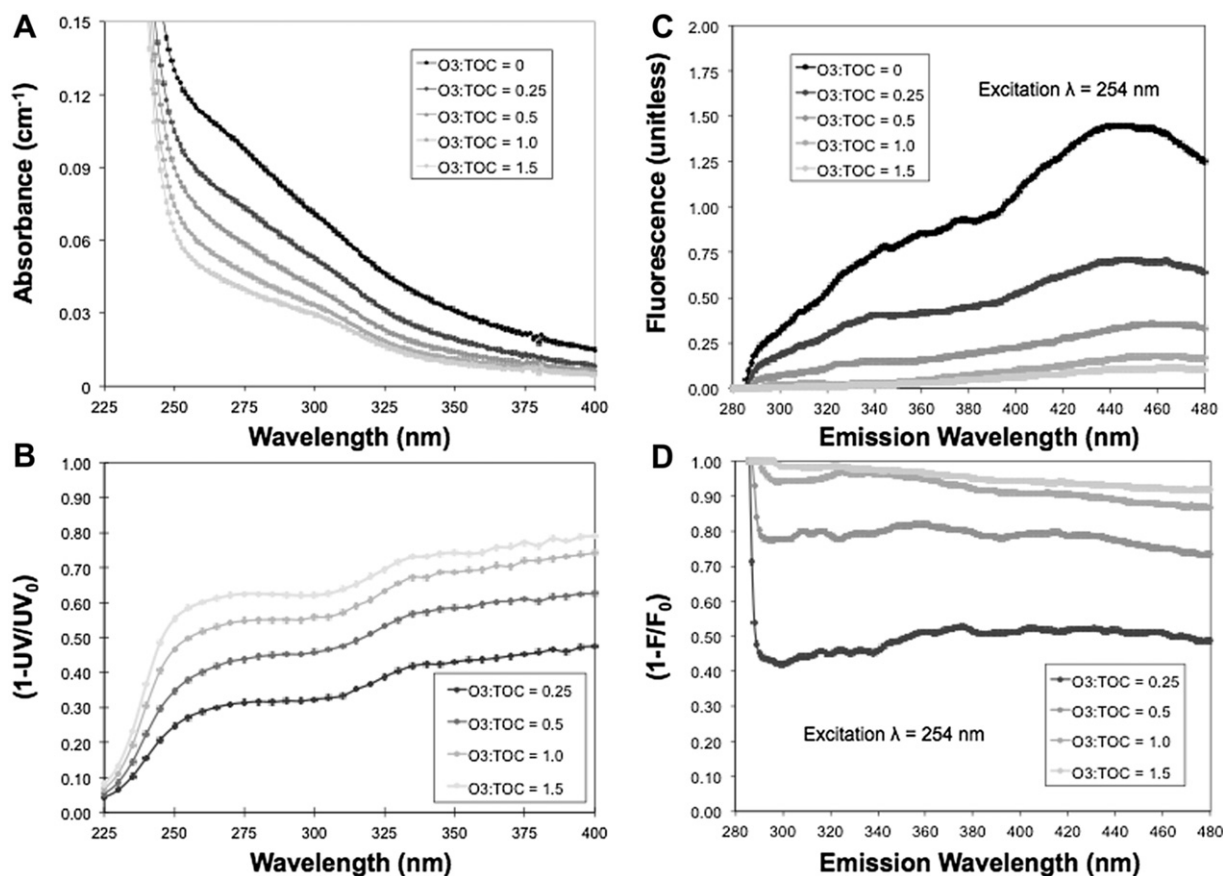

Fig. 1 – Examples of changes in bulk organic matter as a function of ozone dose (O₃:TOC ratio) in CCWRD secondary effluent samples: (A) absorbance spectra, (B) relative differential absorbance spectra, (C) fluorescence spectra (arbitrary fluorescence units) at an excitation wavelength of 254 nm, and (D) relative differential fluorescence spectra at an excitation wavelength of 254 nm.

the final spiking stock. The final stocks generally contained $\sim 10^8$ CFU/100 mL in the sporulated form. All spore samples were heat-shocked at 80 °C (± 5 °C) and 50 rpm for 12 min prior to plating. Samples with higher anticipated concentrations of spores (i.e., >20/mL) were assayed with the pour plate method using molten nutrient agar (1%) supplemented with trypan blue. Lower concentrations of spores were assayed with membrane filtration using 0.45-μm filters and nutrient agar plates supplemented with trypan blue. Plates were counted after 24 h of incubation at 35 °C.

3. Results and discussion

3.1. Selection of surrogate parameters

Analysis of the full absorbance spectra for each sample indicated that ozone and ozone/H_2O_2 resulted in prominent and monotonic decreases in absorbance at all wavelengths. An example is provided for CCWRD in Fig. 1A. These decreases were also highly reproducible with other secondary effluents. The maximum differentials occurred at wavelengths between 250 and 270 nm, and the relative differentials (Fig. 1B; i.e., ΔUV) offered easily decipherable plateaus between 250 and 300 nm. With respect to fluorescence, all major constituents of EfOM (i.e., microbial biopolymers, fulvic-like, and humic-like species) experienced significant reductions in fluorescence, although the rates of transformation differed between the major groups (data not shown). The fluorescence spectra at an excitation wavelength of 254 nm for ozonated CCWRD samples are illustrated in Fig. 1C, and the corresponding relative differential fluorescence spectra (i.e., ΔTF) are illustrated in Fig. 1D. These observations confirm that changes in absorbance and fluorescence reflect the behavior of the entire ensemble of compounds comprising EfOM. Furthermore, these observations support the conclusion that treatment efficacy can theoretically be evaluated based on measurements at practically any wavelength, or in the case of

fluorescence, using any reasonable combination of excitation and emission wavelengths.

One issue that has not been addressed in the literature is the effect of TOrC-specific properties on correlation models. In order to explore this concept in greater detail, the absorbance and fluorescence fingerprints of individual target compounds spiked in deionized water (~ 10 mg/L) were evaluated (Supplementary Information Appendix 1; SI-A1). Preliminary correlations were developed for compound-specific properties (e.g., maximum absorbance wavelength, excitation and emission wavelengths corresponding to maximum fluorescence), but these correlations did not provide any significant benefits over ΔUV$_{254}$ or ΔTF. Based on these observations, there was insufficient evidence to justify selection of compound-specific parameters. Therefore, the empirical correlations described below were based on the bulk organic parameters most commonly discussed in practice (ΔUV$_{254}$) and research (ΔTF).

After aggregating the ΔUV$_{254}$ and ΔTF data from the nine sets of bench-scale experiments (Fig. 2), the reductions in UV$_{254}$ absorbance and total fluorescence were described by the equations below. The models based on a specific H_2O_2:O_3 ratio sometimes provide stronger correlations than the generic model.

$$\text{All } H_2O_2\text{:} O_3\text{: } \Delta UV_{254}(\%) = 100 * 0.46 (O_3\text{:}TOC)^{0.53} \quad R^2 = 0.87 \quad (1)$$

$$\text{All } H_2O_2\text{:} O_3\text{: } \Delta TF(\%) = 100 * 0.83 (O_3\text{:}TOC)^{0.35} \quad R^2 = 0.77 \quad (2)$$

$$H_2O_2\text{:} O_3 = 0\text{: } \Delta UV_{254}(\%) = 100 * 0.51 (O_3\text{:}TOC)^{0.63} \quad R^2 = 0.92 \quad (3)$$

$$H_2O_2\text{:} O_3 = 0\text{: } \Delta TF(\%) = 100 * 0.85 (O_3\text{:}TOC)^{0.37} \quad R^2 = 0.78 \quad (4)$$

$$H_2O_2\text{:} O_3 = 0.5\text{: } \Delta UV_{254}(\%) = 100 * 0.45 (O_3\text{:}TOC)^{0.48} \quad R^2 = 0.90 \quad (5)$$

$$H_2O_2\text{:} O_3 = 0.5\text{: } \Delta TF (\%) = 100 * 0.84 (O_3\text{:}TOC)^{0.33} \quad R^2 = 0.77 \quad (6)$$

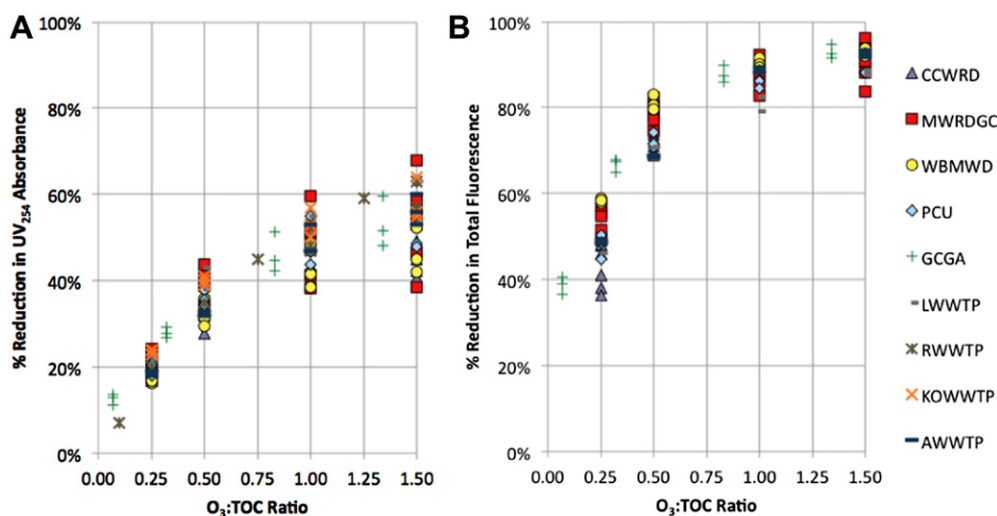$$H_2O_2\text{:} O_3 = 1.0\text{: } \Delta UV_{254}(\%) = 100 * 0.42 (O_3\text{:}TOC)^{0.45} R^2 = 0.86 \quad (7)$$

Fig. 2 – Relative reductions in (A) UV$_{254}$ absorbance (ΔUV$_{254}$) and (B) total fluorescence (ΔTF) for the nine secondary effluents after ozonation (H_2O_2:O_3 = 0–1.0) in the laboratory systems.

$$H_2O_2 : O_3 = 1.0 : \Delta TF(\%) = 100 * 0.81(O_3 : TOC)^{0.35} \quad R^2 = 0.77 \quad (8)$$

3.2. Development of TOrC correlations

The first step in developing the empirical correlation models was to plot the relative elimination of the target compounds (in %) against the relative changes in both UV_{254} absorbance (ΔUV_{254} in %) and total fluorescence (ΔTF in %). Fig. 3 provides examples for sulfamethoxazole and meprobamate, and Appendix SI-A2 provides the remaining scatter plots for each target compound. Each marker represents a single ozone or ozone/H_2O_2 dosing condition. Filtered versus unfiltered (SI-A3) and ozone versus ozone/H_2O_2 samples (SI-A4) were not differentiated in Fig. 3 and SI-A2 because they did not yield noticeably different results. With respect to peroxide addition (SI-A4), several of the plots indicate that $H_2O_2:O_3$ ratios had

a very slight impact on the correlation models, specifically for the more resistant compounds. The addition of H_2O_2 caused slight decreases in process efficacy for reducing UV_{254} absorbance and fluorescence, but the corresponding effects on contaminant concentrations were generally insignificant. Since the impact was minimal, all of the ozone and ozone/ H_2O_2 data were grouped into a single dataset (Fig. 3 and SI-A2) prior to developing the final correlations.

Due to the empirical nature of these correlations, some degree of scatter was anticipated. However, based on the overlapping data points in Fig. 3 and SI-A2, there was no apparent difference between the various water matrices on a compound-specific basis. In contrast, there were dramatic differences between contaminants, which can be explained by their reactivity with ozone and/or •OH (Table 2). Therefore, individual correlations were developed for each target
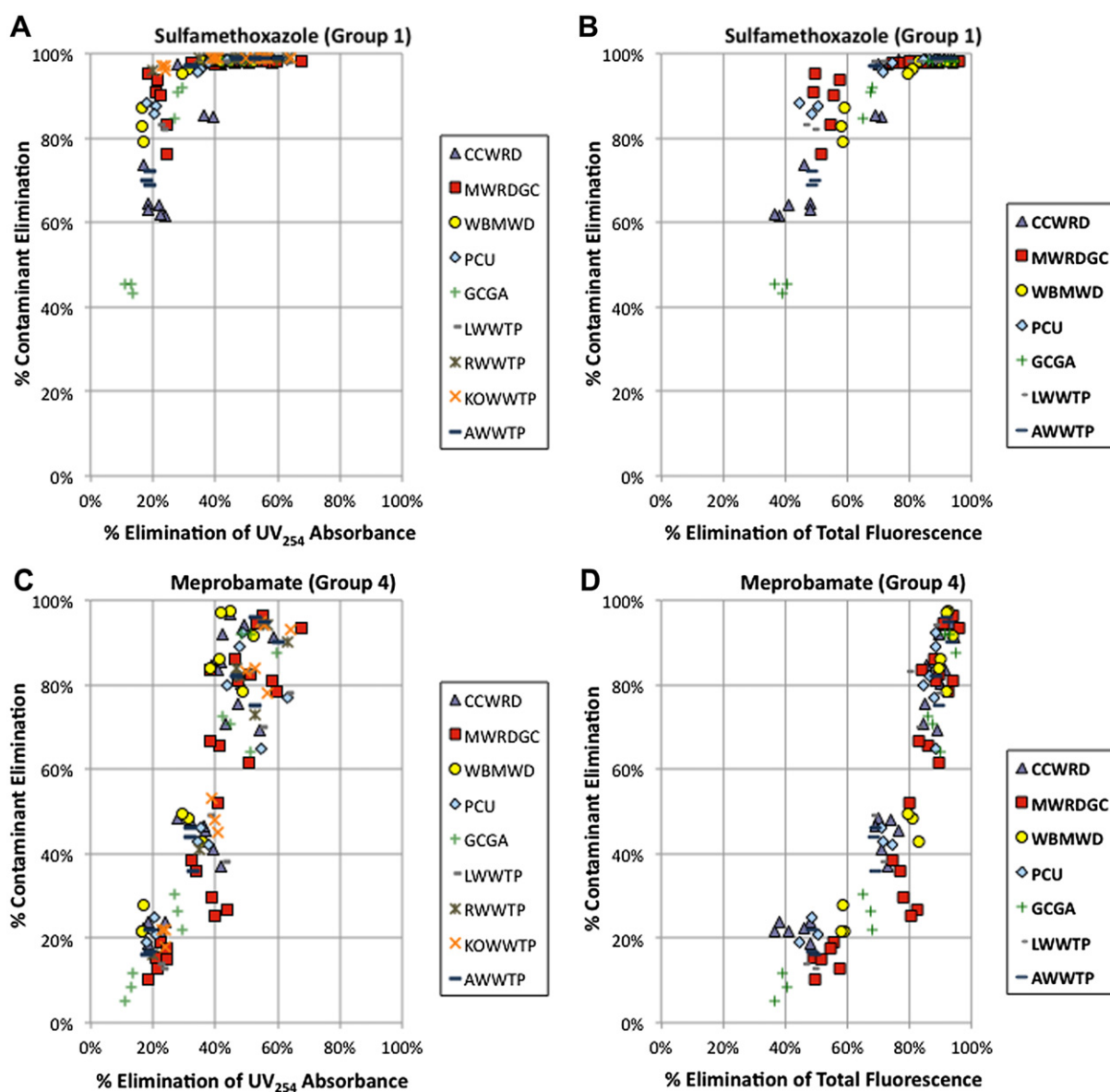

Fig. 3 – Example correlations between the % elimination of (A) UV_{254} absorbance and Group 1 compound sulfamethoxazole, (B) total fluorescence and sulfamethoxazole, (C) UV_{254} absorbance and Group 4 compound meprobamate, and (D) total fluorescence and meprobamate. The remaining correlations are illustrated in SI-A2 through SI-A6.

compound according to Eq. (9), and the corresponding regression parameters are summarized in Table 3. These correlations focus on the linear portion of the decay curves due to practical treatment limitations for most compounds (i.e., maximum practical removal < 99%). For the fast-reacting compounds, the concentrations rapidly approached their respective MRLs even at the lowest O_3:TOC ratio (i.e., nearly vertical lines). Since the data that were <MRL would distort the linear regression analyses, some of the data points were excluded, as indicated by the "N_{UV}" or "N_{TF}" parameter for each compound. The compounds within the same group were treated similarly in order to reduce any artificial biases.

$$\left(1 - \frac{[C]}{[C_0]}\right) * 100(\%) = \text{Slope} * \left[\left(1 - \frac{UV \text{ or } TF}{UV_0 \text{ or } TF_0}\right) * 100(\%)\right] + \text{Intercept} \quad (9)$$

The target compounds were separated into five groups based on their reactivity with ozone and •OH. These differences in reactivity affected the magnitudes of their slopes and vertical intercepts, which will be described below. Table 3

also provides regression parameters for a representative "Indicator" in each group based on all of the constituent compounds combined. Finally, Table 4 summarizes the required removals of the organic surrogate parameters to achieve various treatment thresholds (i.e., 90% removal or the relevant CDPH requirement).

For **Group 1**, the contaminant degradation profiles were so steep, as illustrated in Fig. 3A, that it was not possible to describe the removal rate based on ΔUV_{254} (i.e., $R^2 < 0.2$). Although it was possible to develop correlation models with ΔTF, the correlations were relatively weak (i.e., $R^2 < 0.57$). With respect to the ΔTF models in Table 3, the Group 1 compounds were generally characterized by high slopes (>1.6) with low vertical intercepts (<10) or low slopes (<1.6) with high vertical intercepts (>10). The high slopes indicate rapid reaction rates, as would be expected for these compounds, and the low vertical intercepts indicate that elimination of these particular compounds started at the same time as the elimination of UV_{254} absorbance and total fluorescence. In contrast, the fastest reacting compounds, including triclosan, bisphenol A, and diclofenac, had lower slopes because their oxidation started quicker than that of UV_{254} absorbance and total

Table 3 – Summary of regression parameters.

Contaminant	N_{UV} | N_{TF}	UV$_{254}$ absorbance			Total fluorescence		
		Slope	Intercept	R^2	Slope	Intercept	R^2
Group 1[a]							
Bisphenol A	30 | 26	N/A			1.33	22	0.56
Carbamazepine	30 | 26	N/A			1.72	−3	0.53
Diclofenac	30 | 26	N/A			1.48	12	0.56
Naproxen	30 | 26	N/A			1.74	−4	0.55
Sulfamethoxazole	30 | 26	N/A			1.66	−6	0.54
Triclosan	30 | 26	N/A			1.00	41	0.57
Trimethoprim	30 | 26	N/A			1.60	4	0.50
Indicator	210 | 182	N/A			1.51	10	0.47
Group 2[a]							
Atenolol	60 | 52	2.37	−4	0.79	1.55	−33	0.83
Gemfibrozil	60 | 52	1.80	31	0.62	1.32	0	0.77
Indicator	120 | 104	2.08	13	0.59	1.43	−17	0.68
Group 3[a]							
DEET	60 | 52	1.59	−2	0.67	1.07	−24	0.76
Ibuprofen	60 | 52	1.62	5	0.64	1.15	−20	0.77
pCBA	42 | 42	1.31	3	0.48	0.86	−15	0.54
Phenytoin	60 | 52	1.72	2	0.60	1.16	−22	0.66
Primidone	60 | 52	1.54	−1	0.65	1.05	−22	0.74
Indicator	282 | 250	1.58	1	0.58	1.06	−20	0.65
Group 4[a]							
1,4-Dioxane	40 | 40	1.57	−18	0.69	1.29	−57	0.70
Atrazine	124 | 104	1.79	−21	0.76	1.46	−61	0.80
Meprobamate	124 | 104	1.87	−16	0.64	1.53	−59	0.82
Indicator	288 | 248	1.80	−19	0.74	1.46	−59	0.76
Group 5[a]							
TCEP	121 | 101	0.57	−7	0.56	0.44	−19	0.56
Microbial inactivation[b]							
E. coli	95 | 95	0.13	−1.2	0.47	0.10	−3.6	0.46
MS2	94 | 94	0.14	−0.1	0.71	0.11	−3.4	0.78
Bacillus Spores	15 | 15	N/A	N/A				

N_{UV} and N_{TF} refer to the number of data point used in the development of the regression parameters.
a % compound elimination vs. % organic surrogate elimination (see Eq. (9)).
b Log inactivation vs. % organic surrogate elimination (see Eq. (19)).

Table 4 – Required elimination of organic surrogates to achieve treatment thresholds.

Contaminant	CDPH Group and objective	CDPH objective		90% elimination	
		UV$_{254}$	TF	UV$_{254}$	TF
Group 1					
Bisphenol A	A	69%	~20%	35%	~20%	51%
Carbamazepine	C	69%	~20%	42%	~20%	54%
Diclofenac	D	69%	~20%	39%	~20%	53%
Naproxen	E	69%	~20%	42%	~20%	54%
Sulfamethoxazole	B	69%	~20%	45%	~20%	58%
Triclosan	A	69%	~20%	28%	~20%	49%
Trimethoprim	D	69%	~20%	41%	~20%	54%
Group 2					
Atenolol	D	69%	31%	66%	40%	79%
Gemfibrozil	F	69%	21%	52%	33%	68%
Group 3					
DEET	G	69%	45%	87%	58%	>100%
Ibuprofen	G	69%	40%	77%	52%	96%
pCBA	G	69%	50%	98%	66%	>100%
Phenytoin	G	69%	39%	78%	51%	97%
Primidone	G	69%	45%	87%	59%	>100%
Group 4					
1,4-Dioxane	–	69%	55%	98%	69%	>100%
Atrazine	D	69%	50%	89%	62%	>100%
Meprobamate	H	50%	35%	71%	57%	97%
Group 5					
TCEP	H	50%	>100%	>100%	>100%	>100%

fluorescence, which translated into vertical shifts in the regressions.

The degradation profiles for the **Group 2** compounds were different from the other compound groups, thereby justifying a unique classification, but the reaction rates for the constituent compounds (gemfibrozil and atenolol) also differed by an order of magnitude. This was apparent in the different regression properties in Table 3, but the models still indicated fast reaction rates by either a high slope or vertical intercept. Fewer data points were excluded from the Group 2 analysis due to the greater resistance of these compounds to oxidation. Due to the reduced reactivity, regression analyses for both ΔUV$_{254}$ and ΔTF were possible.

For the **Group 3** compounds, the ΔUV$_{254}$ models consistently had slopes of 1.7 or lower and vertical intercepts <5 (Table 3). Again, this indicates that contaminant oxidation initiated at the same time as the changes in UV$_{254}$ absorbance but at a much faster rate. For the total fluorescence models, the slopes were generally <1.1, while the vertical intercepts were consistently negative (Table 3). Therefore, the Group 3 compounds experienced a lag in oxidation in comparison to reductions in total fluorescence, but the changes then occur at approximately the same rate.

The **Group 4** compounds demonstrated significant lags in oxidation compared to elimination of UV$_{254}$ absorbance and total fluorescence, as indicated by the negative vertical intercepts (Table 3), and the fluorescence models were also characterized by slightly exponential trends (Fig. 3). This is consistent with the group's low to moderate reactivity with ozone and •OH.

As would be expected, TCEP (**Group 5**) was characterized by extremely small slopes and negative intercepts (Table 3), which indicate that TCEP oxidation starts much later and at a much slower rate than changes in UV$_{254}$ absorbance and total fluorescence. TCEP also had one of the weaker correlations, presumably due to its resistance to oxidation. In fact, the oxidation of TCEP failed to reach 40% with the target ozone doses, thereby providing a limited range of reduction to evaluate with linear regression. It is important to note that musk ketone would also be included in Group 5, but it was not possible to quantify this compound during the bench-scale experiments (see Materials and methods). Since musk ketone and TCEP are characterized by similar resistance to oxidation, the regression parameters for musk ketone would likely be similar to those of TCEP. Therefore, ΔUV$_{254}$ and ΔTF are poor surrogates for TCEP and musk ketone in relation to the CDPH framework and the 90% threshold since the required elimination of UV$_{254}$ absorbance and total fluorescence exceeded the bounds of the model (i.e., >100%).

3.3. Modeling •OH exposure with correlations

In addition to estimating transformation of the target compounds, the aforementioned correlations can also be used to estimate overall •OH exposure with ozone or ozone/H$_2$O$_2$. Eq. (10) represents the linear correlation model for pCBA (regression parameters from Table 3), and Eq. (11) illustrates the process for calculating overall •OH exposure based on changes in pCBA concentrations during advanced oxidation. By combining Eqs. (10) and (11), the •OH exposure models in Eqs. (12) and (13) can be derived.

$$\left(1 - \frac{[pCBA]}{[pCBA]_0}\right) * 100(\%) = \text{Slope} * \left[\left(1 - \frac{UV \text{ or } TF}{UV_0 \text{ or } TF_0}\right) * 100(\%)\right] + \text{Intercept} \quad (10)$$

$$\int [\bullet OH]dt(Ms) = \frac{\ln\left(\frac{[pCBA]}{[pCBA]_0}\right)}{-5 \times 10^9 M^{-1}s^{-1}} \quad (11)$$

$$\Delta UV_{254} \text{ Model}: \int [\bullet OH]dt(Ms)$$
$$= \frac{\ln\left(-0.0131 * \left[\left(1 - \frac{UV}{UV_0}\right) * 100(\%)\right] + 0.97\right)}{-5 \times 10^9} \quad (12)$$

$$\Delta TF \text{ Model}: \int [\bullet OH]dt(Ms)$$
$$= \frac{\ln\left(-0.0086 * \left[\left(1 - \frac{TF}{TF_0}\right) * 100(\%)\right] + 1.15\right)}{-5 \times 10^9} \quad (13)$$

Therefore, instead of spiking and analyzing for changes in pCBA concentration, one can use ΔUV$_{254}$ or ΔTF to develop a rough estimate of overall •OH exposure. This method for calculating •OH exposures can then be used to estimate the elimination of recalcitrant TOrCs (i.e., contribution from ozone assumed to be negligible) based on kinetics, particularly for compounds that do not have established correlation models. For example, a 35% reduction in UV$_{254}$ absorbance during ozonation of secondary effluent corresponds to an •OH

exposure of 1.34×10^{-10} Ms based on the aforementioned pCBA model (Eq. (14)).

$$\Delta UV_{254} = 35\% : \int [\cdot OH]dt(Ms) = \frac{\ln(-0.0131*35 + 0.97)}{-5 \times 10^9}$$
$$= 1.34 \times 10^{-10} \text{ Ms} \qquad (14)$$

The corresponding elimination of meprobamate can be estimated directly from its ΔUV_{254} correlation (49%; Table 3 and Eq. (15)) or from kinetics (42%; Eq. (16)–(18)) using a combination of the estimated •OH exposure and the •OH reaction rate constant ($4.0 \times 10^9 \, M^{-1} \, s^{-1}$; see Table 2). Since the reactivity between meprobamate and ozone is low, this reaction can be ignored.

$$\Delta UV_{254} = 35\% : \left(1 - \frac{[C]}{[C_0]}\right)*100(\%) = 1.87*35 - 16 = 49\% \qquad (15)$$

$$\ln(C/C_0) = -(k.OH)\left(\int [\cdot OH]dt\right), \qquad (16)$$

where the contribution from ozone is assumed to be negligible.

$$\ln(C/C_0) = -(4.0 \times 10^9 M^{-1}s^{-1})(1.34 \times 10^{-10}Ms) = -0.54 \qquad (17)$$

$$\left(1 - \frac{[C]}{[C_0]}\right)*100(\%) = (1 - \exp(-0.54))*100(\%) = 42\% \qquad (18)$$

These estimates can be compared to the experimental observations for meprobamate in Fig. 3. The models proposed in Eqs. (12) and (13) represent a first approximation to assess •OH exposure using on-line instrumentation. Additional studies are needed to further validate this approach in pilot- and full-scale systems.

3.4. Development of microbial correlations

The ΔUV_{254} and ΔTF correlations for the target microbes are provided in Table 3 and SI-A2 through SI-A4. In contrast with the target compounds for which the upper bound of

elimination was generally <99%, the microbial correlations were based on log inactivation rather than percent reductions in concentrations, as described in Eq. (19):

$$-\text{Log}\left(\frac{N}{N_0}\right) = \text{Slope}*\left[\left(1 - \frac{UVorTF}{UV_0orTF_0}\right)*100(\%)\right] + \text{Intercept} \qquad (19)$$

Therefore, the slopes and intercepts cannot be compared directly to those of the target compounds. In addition, the correlations for the surrogate microbes generally exhibited greater variability than those of the target compounds, which was also observed in Bahr et al. (2007). It is interesting to note that the inactivation of E. coli and MS2 was quite comparable, which indicates that E. coli could possibly be used as a surrogate for some viruses, but MS2 demonstrated stronger correlations than E. coli (Table 3). With respect to B. subtilis, the spores required extended exposure to ozone before any inactivation was observed (SI-A2 through SI-A4), which is consistent with the lag phase described by Driedger et al. (2001). Therefore, it was not possible to accurately correlate B. subtilis spore inactivation with ΔUV_{254} or ΔTF. In fact, nearly 50% and 90% reductions in UV_{254} absorbance and total fluorescence, respectively, were required before any inactivation was observed, but the inactivation was very rapid after that threshold was achieved.

3.5. Pilot-scale validation

As shown in Fig. 4A, Fig. 4B, and SI-A5, there was relatively good agreement between the bench- (indicated by WRF-09-10 markers) and pilot-scale correlations, which highlights the widespread applicability of this concept to diverse water qualities and treatment scales. As with the bench-scale data, the contaminant correlations proved to be much stronger than the microbial correlations, particularly in the case of E. coli. Therefore, the use of ΔUV_{254} or ΔTF may be limited to general process performance and contaminant oxidation, while disinfection may still require more traditional frameworks (e.g., the CT concept) to describe expected levels of inactivation.
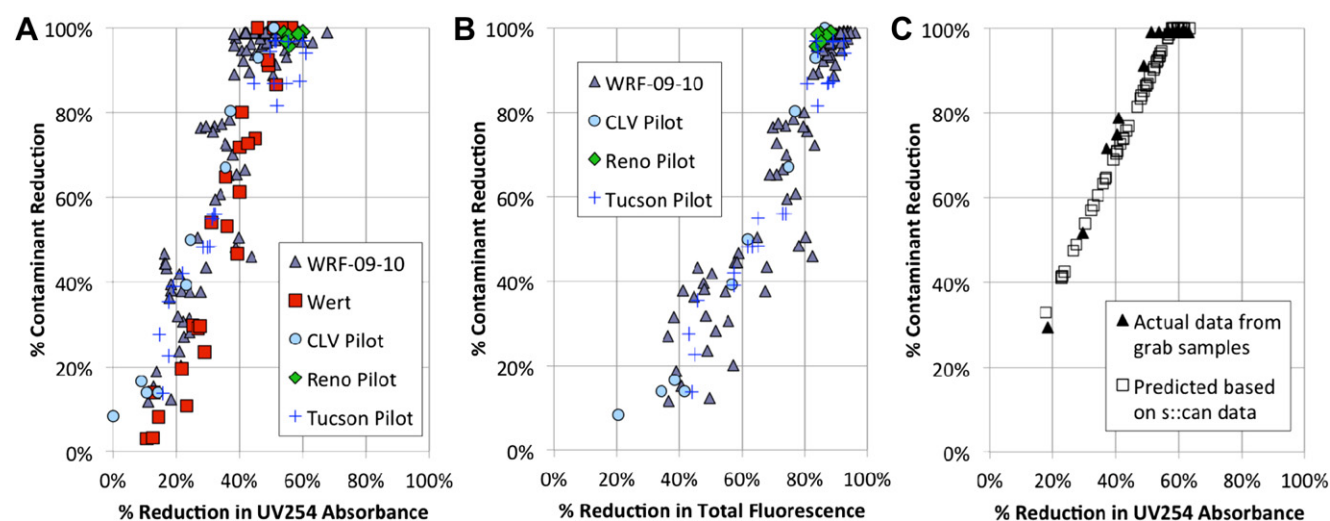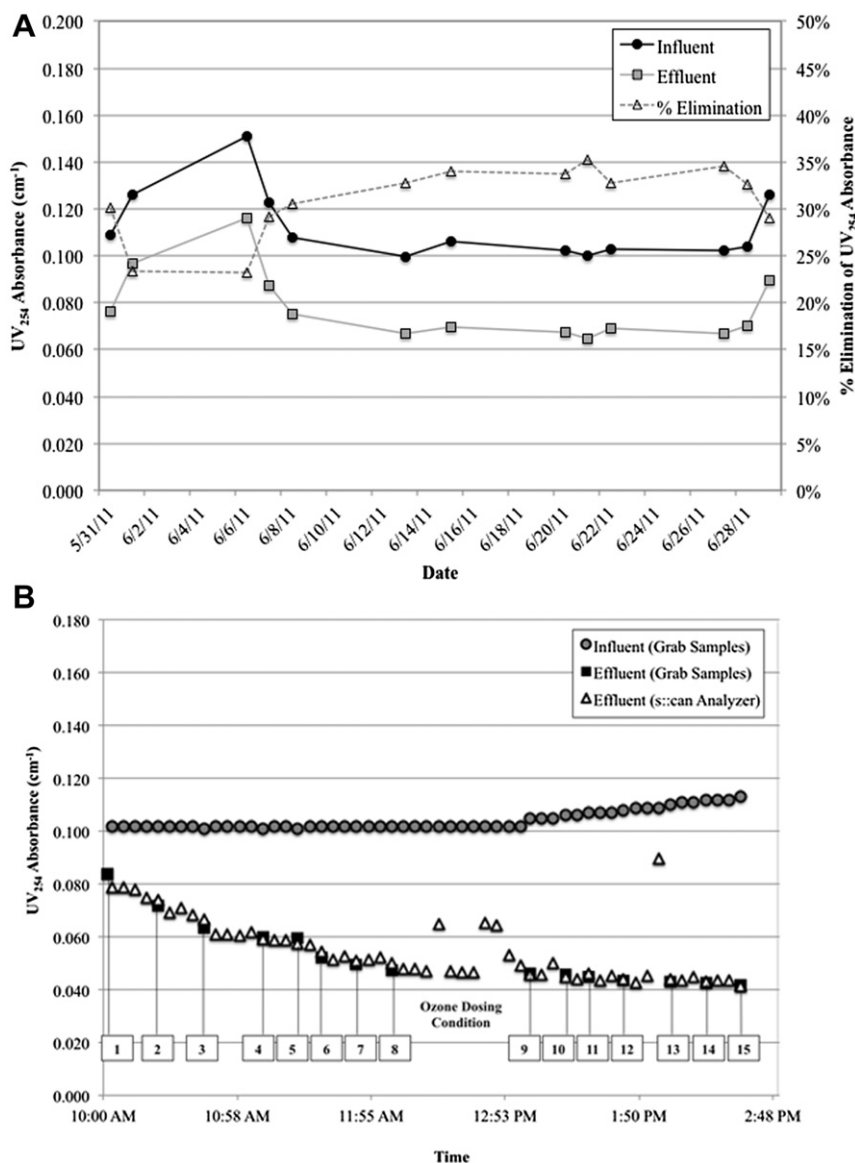

Fig. 4 – Validation of the (A) ΔUV_{254} and (B) ΔTF correlations for phenytoin based on grab samples at the various pilot-scale sites. The validation of the data from the s::can spectro::lyser is illustrated in (C). The remaining pilot-scale validations are illustrated in SI-A5 and SI-A6.

Fig. 5 − (A) Influent and effluent UV_{254} absorbance grab samples from the ozone process at the CLV pilot. **(B)** Comparison of grab samples and online analyzer data for UV_{254} absorbance at the CLV pilot. The ozone dosing conditions (i.e., 1−15) are described in **Table S1.**

With respect to the CLV pilot, a series of grab samples was collected to evaluate the continuous operation of the ozone pilot and validate the data from the online UV_{254} absorbance analyzer. Fig. 5A illustrates the temporal variability in UV_{254} absorbance prior to and after ozonation in addition to the corresponding differentials. Although the UV_{254} absorbance prior to ozonation fluctuated over time, the constant ozone dose applied during this period (1.5 mg/L; O_3:TOC = 0.25; H_2O_2:O_3 = 0) resulted in a consistent ΔUV_{254} of approximately 30%.

In addition to the grab samples in Fig. 5A, Fig. S2A illustrates the fluctuation in UV_{254} absorbance for the MBR filtrate prior to ozonation, which was continuously monitored from May 21st through May 31st of 2011 with the online analyzer. The grab sample toward the end of the monitoring period was used as a preliminary validation between the online analyzer

and laboratory data. Fig. S2B illustrates the continuous monitoring data for the ozonated MBR filtrate from May 31st to July 4th of 2011. In contrast with the relatively stable signal before ozonation, the signal after ozonation experienced rapid fluctuations due to analyzer interference. In order to improve the clarity of the data, any erroneous values >0.100 cm^{-1} were removed from the data set and attributed to the following reasons: unexpected or planned shutdowns of the pilot systems, scaling or biological fouling of the analyzer, and periodic spikes in turbidity or air bubbles that interrupted the light path in the flow cell. Ensuring continuous flow through the analyzer and implementing a routine cleaning and maintenance schedule (e.g., daily instead of weekly) would likely be required to mitigate these problems in the future. However, this preliminary data set indicates that online

monitoring of UV_{254} absorbance is a promising operational tool.

In addition to the long-term monitoring data, a one-day, variable ozone dose experiment was also performed to validate the empirical TOrC correlations. Fig. 5B illustrates the resulting data from both grab and continuous monitoring samples, where the numbered boxes represent different dosing conditions ($O_3 = 0.6$–9.0 mg/L; O_3:TOC $= 0.1$–2.0; see Table S1 for details). During the short timeframe of the variable dose experiment, the influent water quality (shaded circles) was relatively stable, and the data demonstrate good consistency between the online (empty triangles) versus grab sample (black squares) data. Fig. 4C and SI-A6 illustrate the use of these grab samples and online data to validate the TOrC correlations.

With the exception of ibuprofen and TCEP, the predictive model based on the online absorbance readings and the actual levels of transformation based on the grab samples were consistent. This was particularly true for the highly susceptible Group 1 compounds, which were almost always <MRL after oxidation, but the data were also relatively consistent for the Group 2, 3, and 4 compounds. It is unclear exactly why the actual data and the predictive model for ibuprofen and TCEP were dissimilar. However, the bench-scale TCEP data that were used to develop the correlations also showed more variability than the other compounds. In general, the predictive model tended to overestimate the level of oxidation for some compounds.

3.6. Full-scale validation

The full-scale samples indicated that the reductions in UV_{254} absorbance, total fluorescence, and many of the target compounds at the full-scale facility were similar to the predicted values (Table 5). Exclusions include compounds that were not detected in the ozone influent sample, which were omitted from Table 5; compounds that reached their respective MRLs during ozonation, which limited the quantifiable range; and two specific outliers (DEET and E. coli).

Ozonation only achieved 45% elimination of DEET, but it is unclear what caused this deviation from the bench-scale correlation. With respect to E. coli, the potential level of inactivation was limited to only 3.5 logs since the ozone influent sample only contained 3.5×10^3 MPN/100 mL. It is easier to achieve several orders of magnitude of inactivation when the initial E. coli level is high, such as in a spiked bench-scale experiment, but it becomes increasingly difficult to inactivate bacteria as the numbers approach the detection limit of the assay, possibly due to shielding. This may be one possible explanation for the discrepancy between the maximum level of inactivation (3.5 logs) and the observed level of inactivation (2.5 logs). With the exception of these two outliers, the models provided relatively accurate predictions of process performance, which highlights the utility of this surrogate framework as an alternative to frequent TOrC monitoring.

4. Conclusions

One of the critical components of treatment plant operation is real-time monitoring of process performance that allows for subsequent operational adjustments. As such, the primary goal of this study was to provide operators with tools to predict treatment efficacy and identify breakdowns and inefficiencies in the performance of oxidation processes that rely heavily on fast reacting oxidants, such as ozone and •OH. In order to better integrate ozonation and other AOPs into water

Table 5 – Full-scale validation of UV_{254} absorbance and total fluorescence correlations.

Parameter	Ozone influent	Ozone effluent	Actual elimination	ΔUV_{254} prediction	ΔTF prediction
Organic Surrogates					
UV_{254} Absorbance	0.116 cm^{-1}	0.059 cm^{-1}	49%	51%	N/A
Total Fluorescence	28,782 (unitless)	4546 (unitless)	84%	N/A	85%
Group 1					
Carbamazepine	220 ng/L	<10 ng/L	<MRL[a]	>99%	>99%
Diclofenac	47 ng/L	<25 ng/L	<MRL[a]	>99%	>99%
Naproxen	26 ng/L	<25 ng/L	<MRL[a]	>99%	>99%
Sulfamethoxazole	2200 ng/L	< 25 ng/L	<MRL[a]	>99%	>99%
Trimethoprim	21 ng/L	< 10 ng/L	<MRL[a]	>99%	>99%
Group 2					
Atenolol	190 ng/L	<25 ng/L	<MRL[a]	>99%	96%
Gemfibrozil	72 ng/L	<10 ng/L	<MRL[a]	>99%	>99%
Group 3					
DEET	100 ng/L	55 ng/L	45%	76%	65%
Phenytoin	150 ng/L	17 ng/L	89%	86%	74%
Primidone	210 ng/L	45 ng/L	79%	74%	65%
Group 4					
Meprobamate	350 ng/L	110 ng/L	69%	76%	68%
Group 5					
TCEP	410 ng/L	340 ng/L	17%	21%	18%
Microbes					
E. coli	3.5×10^3 MPN/100 mL	12 MPN/100 mL	2.5 logs[a]	5.2 logs	4.7 logs

a % elimination or log inactivation limited by MRL.

and wastewater treatment, a more comprehensive understanding of the available technologies in addition to tools that make them amenable to the current regulatory framework are required. Equipping utilities and operators with quick and simple proxies to assess oxidation and disinfection efficacy will reduce the analytical demand related to continuous monitoring of trace organic contaminants and microorganisms, allow for rapid adjustments to operational variables (e.g., ozone and/or H_2O_2 dose), and provide a basis for awarding removal credits for various contaminants.

This study provides quantitative information that can be used to tailor a surrogate framework for indicator compounds to an individual system, similar to what is now required by the California Department of Public Health. Differential UV_{254} absorbance and total fluorescence were correlated with trace organic contaminant oxidation and microbial inactivation to provide estimates of treatment efficacy in 17 different wastewater matrices from the U.S., Switzerland, and Australia. The results of this study indicate that ΔUV_{254} and ΔTF can be used as surrogates for target compound elimination. The primary benefit of this strategy is that it requires minimal equipment, expertise, time, and cost compared to full-scale monitoring of target compounds and pathogens. Automated online analyzers are available for UV absorbance and fluorescence so full-scale implementation of the empirical models developed in this study is entirely feasible. Although there is a certain amount of inherent variability in the models, the pilot- and full-scale validation efforts indicate that the models are robust. As mentioned earlier, similar models can be applied to other forms of advanced oxidation, such as UV/H_2O_2, so expanded model databases are also warranted for other forms of treatment. Future research should also attempt to develop empirical models based on reaction rate constants with ozone and ·OH.

With respect to microbial inactivation, the correlations may not yet be strong enough to warrant disinfection credits, particularly for microbes with significant lag phases (e.g., *B. subtilis* spores and *Cryptosporidium* oocysts), but the models still provide a useful estimate of expected log inactivation for some bacteria and viruses. Additional studies would be necessary to further refine the microbial inactivation models and integrate them into a regulatory framework.

Acknowledgments

Appendix A. Supplementary data

Supplementary data related to this article can be found at http://dx.doi.org/10.1016/j.watres.2012.08.037.

REFERENCES

Acero, J.L., Stemmler, K., von Gunten, U., 2000. Degradation kinetics of atrazine and its degradation products with ozone and OH radicals: a predictive tool for drinking water treatment. Environmental Science and Technology 34, 591–597.

Adams, M., 1959. Bacteriophages. Book Bacteriophages. Interscience Publishers, New York.

Bahr, C., Schumacher, J., Ernst, M., Luck, F., Heinzman, B., Jekel, M., 2007. SUVA as control parameter for the effective ozonation of organic pollutants in secondary effluent. Water Science and Technology 55, 267–274.

Benner, J., Salhi, E., Ternes, T., von Gunten, U., 2008. Ozonation of reverse osmosis concentrate: kinetics and efficiency of beta blocker oxidation. Water Research 42, 3003–3012.

Bowman, R.H., Miller, P., Purchase, M., Schoellerman, R., 2001. Ozone-peroxide Advanced Oxidation Water Treatment System for Treatment of Chlorinated Solvents and 1,4-dioxane. American Chemical Society National Meeting, San Diego, CA.

Buffle, M., Schumacher, J., Meylan, S., Jekel, M., von Gunten, U., 2006. Ozonation and advanced oxidation of wastewater: effect of O_3 dose, pH, DOM and HO• scavengers on ozone decomposition and HO• generation. Ozone Science & Engineering 28, 247–259.

Burns, N., Hunter, G., Jackman, A., Hulsey, B., Coughenour, J., Walz, T., 2007. The return of ozone and the hydroxyl radical to wastewater disinfection. Ozone Science & Engineering 29, 303–306.

Camacho-Munoz, D., Martin, J., Santos, J.L., Aparicio, I., Alonso, E., 2009. An affordable method for the simultaneous determination of the most studied pharmaceutical compounds as wastewater and surface water pollutants. Journal of Separation Science 32, 3064–3073.

CDPH, 2011. Groundwater Replenishment Reuse. Draft Regulations. Title 22 California Code of Regulations. California Department of Public Health.

Chen, W., Westerhoff, P., Leenheer, J.A., Booksh, K., 2003. Fluorescence excitation-emission matrix regional integration to quantify spectra for dissolved organic matter. Environmental Science and Technology 37, 5701–5710.

Deborde, M., Rabouan, S., Duguet, J., Legube, B., 2005. Kinetics of aqueous ozone-induced oxidation of some endocrine disruptors. Environmental Science and Technology 39, 6086–6092.

Dickenson, E.R.V., Drewes, J.E., Sedlak, D.L., Wert, E.C., Snyder, S.A., 2009. Applying surrogates and indicators to assess removal efficiency of trace organic chemicals during chemical oxidation of wastewaters. Environmental Science and Technology 43, 6242–6247.

Dodd, M.C., Buffle, M., von Gunten, U., 2006. Oxidation of antibacterial molecules by aqueous ozone: moiety-specific reaction kinetics and application to ozone-based wastewater treatment. Environmental Science and Technology 40, 1969–1977.

Dodd, M.C., Kohler, H.P.E., von Gunten, U., 2009. Oxidation of antibacterial compounds by ozone and hydroxyl radical: elimination of biological activity during aqueous ozonation

processes. Environmental Science and Technology 43, 2498–2504.

Driedger, A., Staub, E., Pinkernell, U., Marinas, B., Koster, W., von Gunten, U., 2001. Inactivation of Bacillus subtilis spores and formation of bromate during ozonation. Water Research 35, 2950–2960.

Gerrity, D., Gamage, S., Holady, J.C., Mawhinney, D.B., Quinones, O., Trenholm, R.A., Snyder, S.A., 2011a. Pilot-scale evaluation of ozone and biological activated carbon for trace organic contaminant mitigation and disinfection. Water Research 45, 2155–2165.

Gerrity, D., Snyder, S., 2011. Review of ozone for water reuse applications: toxicity, regulations, and trace organic contaminant oxidation. Ozone Science & Engineering 33, 253–266.

Gerrity, D., Stanford, B.D., Trenholm, R.A., Snyder, S.A., 2010. An evaluation of a pilot-scale nonthermal plasma advanced oxidation process for trace organic compound degradation. Water Research 44, 493–504.

Gerrity, D., Trenholm, R.A., Snyder, S.A., 2011b. Temporal variability of pharmaceuticals and illicit drugs in wastewater and the effects of a major sporting event. Water Research 45, 5399–5411.

Hoigne, J., Bader, H., 1994. Characterization of water quality criteria for ozonation processes. Part II: lifetime of added ozone. Ozone Science & Engineering 16, 121–134.

Hollender, J., Zimmermann, S.G., Koepke, S., Krauss, M., McArdell, C.S., Ort, C., Singer, H., von Gunten, U., Siegrist, H., 2009. Elimination of organic micropollutants in a municipal wastewater treatment plant upgraded with a full-scale post-ozonation followed by sand filtration. Environmental Science and Technology 43, 7862–7869.

Huber, M.M., Canonica, S., Park, G.Y., von Gunten, U., 2003. Oxidation of pharmaceuticals during ozonation and advanced oxidation processes. Environmental Science and Technology 37, 1016–1024.

Huber, M.M., Gobel, A., Joss, A., Hermann, N., Loffler, D., McArdell, C.S., Ried, A., Siegrist, H., Ternes, T.A., von Gunten, U., 2005. Oxidation of pharmaceuticals during ozonation of municipal wastewater effluents: a pilot study. Environmental Science and Technology 39, 4290–4299.

Huber, M.M., Ternes, T.A., von Gunten, U., 2004. Removal of estrogenic activity and formation of oxidation products during ozonation of 17α-ethinylestradiol. Environmental Science and Technology 38, 5177–5186.

Kaiser, H.P., Koster, O., Gresch, M., Perissef, P. Jaggi, P., Salhi, E., von Gunten, U. Process control of ozonation systems: a novel real-time approach. Ozone: Science and Engineering, submitted for publication.

Katsoyiannis, I.A., Canonica, S., von Gunten, U., 2011. Efficiency and energy requirements for the transformation of organic micropollutants by ozone, ozone/H_2O_2 and UV/H_2O_2. Water Research 45, 3811–3822.

Lee, Y., Escher, B.I., von Gunten, U., 2008. Efficient removal of estrogenic activity during oxidative treatment of waters containing steroid estrogens. Environmental Science and Technology 42, 6333–6339.

Lee, Y., von Gunten, U., 2012. Quantitative Structure-Activity Relationships (QSARs) for the transformation of organic micropollutants during oxidative water treatment. Water Research 46, 6177–6195.

Mesquita, M.M.F., Stimson, J., Chae, G.-T., Tufenkji, N., Ptzcek, C.J., Blowes, D.W., Emelko, M.B., 2010. Optimal preparation and purification of PRD1-like bacteriophages for use in environmental fate and transport studies. Water Research 44, 1114–1125.

Nanaboina, V., Korshin, G.V., 2010. Evolution of absorbance spectra of ozonated wastewater and its relationship with the degradation of trace-level organic species. Environmental Science and Technology 44, 6130–6137.

Packer, J.L., Werner, J.J., Latch, D.E., McNeill, K., Arnold, W.A., 2003. Photochemical fate of pharmaceuticals in the environment: Naproxen, diclofenac, clofibric acid, and ibuprofen. Aquatic Science 65, 342–351.

Pisarenko, A.N., Stanford, B.D., Yan, D., Gerrity, D., Snyder, S.A., 2012. Effects of ozone and ozone/peroxide on trace organic contaminants and NDMA in drinking water and water reuse applications. Water Research 46, 316–326.

Razavi, B., Song, W., Cooper, W.J., Greaves, J., Jeong, J., 2009. Free-radical-induced oxidative and reductive degradation of fibrate pharmaceuticals: kinetic studies and degradation mechanisms. The Journal of Physical Chemistry A 113, 1287–1294.

Real, F.J., Javier Benitez, F., Acero, J.L., Sagasti, J.J.P., Casas, F., 2009. Kinetics of the chemical oxidation of the pharmaceuticals primidone, ketoprofen, and diatrizoate in ultrapure and natural waters. Industrial and Engineering Chemistry Research 48, 3380–3388.

Reungoat, J., Escher, B.I., Macova, M., Argaud, F.X., Gernjak, W., Keller, J., 2012. Ozonation and biological activated carbon filtration of wastewater treatment plant effluents. Water Research 46, 863–872.

Reungoat, J., Macova, M., Escher, B.I., Carswell, S., Mueller, J.F., Keller, J., 2010. Removal of micropollutants and reduction of biological activity in a full scale reclamation plant using ozonation and activated carbon filtration. Water Research 44, 625–637.

Rosario-Ortiz, F.L., Wert, E.C., Snyder, S.A., 2010. Evaluation of UV/H_2O_2 treatment for the oxidation of pharmaceuticals in wastewater. Water Research 44, 1440–1448.

Rosenfeldt, E.J., Linden, K.G., 2004. Degradation of endocrine disrupting chemicals bisphenol A, ethinyl estradiol, and estradiol during UV photolysis and advanced oxidation processes. Environmental Science and Technology 38, 5476–5483.

Song, W., Cooper, W.J., Peake, B.M., Mezyk, S.P., Nickelsen, M.G., O'Shea, K.E., 2009. Free-radical induced oxidative and reductive degradation of N, N-diethyl-meta-toluamide (DEET): kinetic studies and degradation pathways. Water Research 43, 635–642.

Stalter, D., Magdeburg, A., Oehlmann, J., 2010a. Comparative toxicity assessment of ozone and activated carbon treated sewage effluents using an in vivo test battery. Water Research 44, 2610–2620.

Stalter, D., Magdeburg, A., Weil, M., Knacker, T., Oehlmann, J., 2010b. Toxication or detoxication? In vivo toxicity assessment of ozonation as advanced wastewater treatment with the rainbow trout. Water Research 44, 439–448.

Suarez, S., Dodd, M.C., Omil, F., von Gunten, U., 2007. Kinetics of triclosan oxidation by aqueous ozone and consequent loss of antibacterial activity: relevance to municipal wastewater ozonation. Water Research 41, 2481–2490.

Thurston-Enriquez, J.A., Haas, C.N., Jacangelo, J., Riley, K., Gerba, C.P., 2003. Inactivation of feline calicivirus and adenovirus type-40 by UV radiation. Applied and Environmental Microbiology 69, 577–582.

Trenholm, R.A., Vanderford, B.J., Snyder, S.A., 2009. On-line solid phase extraction LC-MS/MS analysis of pharmaceutical indicators in water: a green alternative to conventional methods. Talanta 79, 1425–1432.

Vanderford, B.J., Rosario-Ortiz, F.L., Snyder, S.A., 2007. Analysis of p-chlorobenzoic acid in water by liquid chromatography-tandem mass spectrometry. Journal of Chromatography 1164, 219–223.

von Sonntag, C., von Gunten, U., 2012. Chemistry of ozone in water and wastewater treatment: From basic principles to applications. IWA Publishing, London.

Watts, M.J., Linden, K.G., 2009. Advanced oxidation kinetics of aqueous trialkyl phosphate flame retardants and plasticizers. Environmental Science and Technology 43, 2937–2942.

Wert, E.C., Rosario-Ortiz, F.L., Snyder, S.A., 2009a. Effect of ozone exposure on the oxidation of trace organic contaminants in wastewater. Water Research 43, 1005–1014.

Wert, E.C., Rosario-Ortiz, F.L., Snyder, S.A., 2009b. Using ultraviolet absorbance and color to assess pharmaceutical oxidation during ozonation of wastewater. Environmental Science and Technology 43, 4858–4863.

Yuan, F., Hu, C., Hu, X., Qu, J., Yang, M., 2009. Degradation of selected pharmaceuticals in aqueous solution with UV and UV/H_2O_2. Water Research 43, 1766–1774.

Zimmermann, S.G., Wittenwiler, M., Hollender, J., Krauss, M., Ort, C., Siegrist, H., von Gunten, U., 2011. Kinetic assessment and modeling of an ozonation step for full-scale municipal wastewater treatment: micropollutant oxidation, by-product formation and disinfection. Water Research 45, 605–617.